Small-Molecule Screening and Profiling by Using Automated Microscopy

Timothy J. Mitchison*[a]

Automated fluorescence microscopy provides a powerful tool for analyzing the physiological state of single cells with high throughput and high information content. Here I discuss two types of experiments in which this technology was used to discover and characterize bioactive small molecules. In phenotypic-screening experiments, the goal is to find "hits" with specific effects on cells by screening large libraries of small molecules. An example is screening for small molecules that perturb mitosis by novel mechanisms. In cytological-profiling experiments, the goal is to characterize the bioactivity of a limited number of small molecules in considerable depth, and thus understand their mechanism and toxicities at the cellular level. I discuss an example in which 100 small molecules with known bioactivity were profiled by using multiple fluorescent probes, and clustered into mechanistic classes by automated statistical analysis.

Introduction

One of the most powerful tools in cell-biological research is the fluorescence microscope. When combined with appropriate fluorescent probes, this instrument measures the amount and location of specific biomolecules in cells. The resulting information has been central to developing our current understanding of molecular mechanism in cell biology. It is thus natural to use fluorescence microscopy as a tool in the discovery and characterization of biologically active small molecules. In this article, I will discuss two ways we have done this at the Institute of Chemistry and Cell Biology (ICCB): phenotypic screening and cytological profiling. Both applications require collecting and analyzing of images of cells from large numbers of individual experiments, and thus call for automation of both image capture and image analysis. The outline of a typical automated microscopy experiment is shown in Figure 1. Instrumentation for automated microscopy has only recently been introduced, and there have been relatively few publications on this method. For recent reviews that focus on the use of automated microscopy in small molecule discovery see refs. [1–3].

Phenotypic Screening

A central goal of ICCB has been to discover small molecules with novel mechanisms of biological action, which can be used as tools in cell-biology research, and to catalyze therapeutic drug discovery by industry groups. Our main tool has been to screen large libraries of drug-like, and natural product-like, small molecules. We have used a combination of pure protein and biochemical screens, and phenotypic screens in which we assayed for specific alterations to cell physiology. In phenotypic screens, cells or small organisms are cultured in 384-well plates and treated with small molecules. After a time interval appropriate for the biology, each well is scored for the desired physiological change. This method requires the active small molecules ("hits") to be cell-permeable, to be active in the context of the cell environment, and to exhibit some degree of specificity in their biological actions. It can also be used to target proteins that might be unknown or cannot be assayed in pure form. The main disadvantage of phenotypic screening is that the target(s) of the hit molecule must be determined ("target ID"); this can be time consuming and unpredictable. Because of its conceptual similarity to classic genetic screening, phenotypic screening combined with target ID is sometimes called "forwards chemical genetics".[4]

Automated fluorescence microscopy provides a powerful tool for phenotypic screening. Fluorescence microscopy with appropriate probes has the capability to quantify essentially any physiological change that occurs at the single-cell level. Furthermore it can reveal, in the same assay well, undesired or unexpected effects, including toxicity and interesting changes in cell physiology that were not anticipated in the design of the screen. Because of this potentially large information content, screening by automated microscopy is sometimes referred to as "high-content" screening (e.g. ref. [3]). Fluorescence microscopy is also highly sensitive in the sense that small numbers of cells can be used, and biomolecules present at low concentration can be detected.

Figure 2 shows a representative phenotypic screen for small molecules that perturb mitosis. We initiated this screen in a plate reader format, using a luminescent immunoassay for measuring mitotic index. This led to the discovery of monastrol, an inhibitor of the mitotic kinesin Eg5.[5] Monastrol was the first small molecule known to arrest cells in mitosis by a mechanism other than poisoning microtubules, and potent Eg5 inhibitors are now in clinical trials for cancer treatment. We appreciated the potential for an automated microscopy version of the mitosis screen when we observed mitotic arrest as an unanticipated effect in a screen for inhibitors of cell migration.[6] That screen used microscopy of fixed cells migrating

[a] *Prof. T. J. Mitchison*
Dept. Systems Biology and Institute of Chemistry and Cell Biology
Harvard Medical School, Boston, MA 02115 (USA)
Fax: (+1) 617-432-3702
E-mail: timothy_mitchison@hms.harvard.edu

 DOI: 10.1002/cbic.200400272

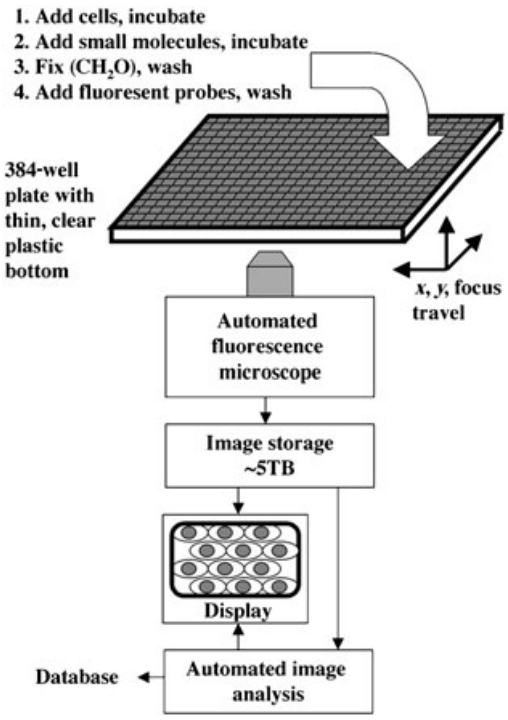

Figure 1. *Schematic of an automated microscopy experiment. Cells are added to 384-well, clear-bottom, microtiter plates in medium and cultured overnight to allow attachment. Small molecules are added from DMSO stock solutions by pin transfer. Final concentration of small molecule is ~30 μM for screening, or a dilution series for profiling. The cells are incubated for a time appropriate for the desired biological changes to occur, typically 1–24 h. A cross-linking fixative (typically formaldehyde in aqueous buffer) is added to stop the biological process and immobilize cell proteins. After a wash that includes detergent to permeabilize cell membranes, fluorescent probes are added. These typically include a blue-fluorescing DNA dye and antibodies to cell proteins that are detected by secondary antibodies labeled with green or red fluorochromes. After a wash, the plate is imaged in each fluorescent channel, or may be stored for several weeks at 4°C. Images are captured by using an automated fluorescence microscope equipped with x, y drives and automated focus, and stored. Images are then scored by eye for desired and undesired/unexpected biological effects, or automated image analysis is used to measure parameters that describe the cell state.*

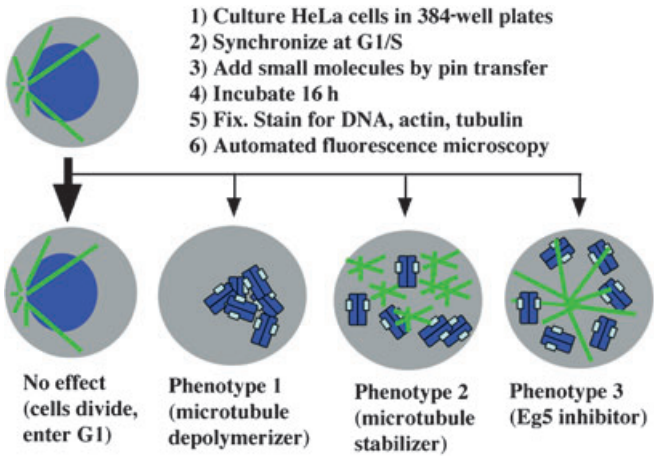

Figure 2. *Phenotypic screen for small molecules that perturb mitosis. HeLa (human cancer) cells were synchronized in G1/S in bulk by using a standard double thymidine block protocol. They were plated into clear-bottom 384-well plates during the second thymidine treatment, released into fresh medium, and small molecules were added to a final concentration of ~30 μM by pin transfer of stock solutions in DMSO. They were fixed 16 h later, sufficient time for unaffected cells to progress through S, G2, M, and cytokinesis into G1 of the next cell cycle. Compounds that disrupt mitosis tend to activate the spindle check point, and arrest the cells in M. The phenotypic effect of mitosis-arresting compounds was scored by eye on the basis of DNA, tubulin, and actin staining. To date, three mitotic-arrest phenotypes have been characterized at the molecular level: 1) lack of microtubules due to inhibition of tubulin, 2) microtubule aggregates due to stabilization of microtubules, and 3) monopolar spindle formation due to Eg5 inhibition. See refs. [5–7].*

Table 1. *A sample of phenotypic screens of small molecule libraries by using automated microscopy run at ICCB.*

Biology	Outline of method	Ref.
Mitotic spindle	See Figure 2	[7]
Cytokinesis	Add SMs for 20 h.[a,b] Stain for DNA, total cytoplasm. Score for binucleate cells.	[8]
Centrosome duplication	Add SMs to cells in hydroxyurea. Stain for γ tubulin, DNA, actin. Score for number of centrosomes.	[9]
Cell migration	Wound cell monolayer, add SMs,[a] fix after 6 h. Stain for DNA, actin. Score by morphology of the wound margin.	[6]
Secretory pathway	Express VSV-G(ts)-GFP fusion. Accumulate in ER at 39°C, Release at 32°C. Score by GFP localization.	[10]
NFAT pathway	Express NFAT-GFP, add SMs,[a] followed by ionomycin to trigger pathway; fix. Score for fraction of signal in the nucleus.	[11]
Nuclear export	Express FOXO1-GFP in cells lacking PTEN. Add SMs,[a] incubate, Fix. Score for fraction of signal in the nucleus.	[12]

[a] SM = small molecules. [b] A genome-wide RNAi library was screened in parallel, 36 h incubation.

into a wound that were fixed and stained for actin and DNA. Mitosis inhibitors revealed themselves by causing cell rounding in the actin image. That experience illustrates the power of microscopy to reveal interesting, unexpected effects, due to its high information content. The automated microscopy version of the mitosis screen was used to discover a new, more potent Eg5 inhibitor,[7] and we are currently using it to find and characterize small molecules that perturb mitosis by additional mechanisms.

A number of phenotypic screens of small molecule libraries by automated microscopy have been run at ICCB (Table 1). Most of the screens in Table 1 were scored by eye, and thus gave a relatively qualitative measure of physiological change induced by small molecules. This reflects the challenges in developing robust image-analysis algorithms, and a desire from biologists to get the result quickly. Quantifying physiological changes at the single-cell level by automated microscopy remains a challenge, though it will become easier as automated microscopes improve in terms of reliable automatic focusing and better signal-to-noise ratios in images. Commercial software is now available for standard image-analysis tasks, such as quantifying the amount of fluorescence per cell, nuclear import etc., and for some more sophisticated tasks, such as

scoring morphology and cytotoxicity. However, it is an ongoing research challenge to determine how much information relevant to small-molecule effects is contained in images of cells and how this information can be automatically extracted. Examples of automated scoring of imaging data are described in refs. [9,13], and I will discuss a new approach to broadly extracting relevant information below.

Cytological Profiling

It became evident from our screening projects that fluorescent images of cells contained far more information than that we were actually using to score the screen. This point was exemplified when we used small molecules with known mechanisms to calibrate cell responses in a centrosome-duplication screen.[9] Those observations prompted the question, how much information on cell physiology is present in fluorescence images of cells, and how can we extract this information to understand the phenotypic effect of a small molecule? To begin addressing this question systematically, we developed a cytological-profiling approach.[14] Use of automated microscopy to profile small-molecule action had been investigated previously by using a limited number of probes and scoring for expected cell effects.[9,13,15] Our idea was to use a larger number of probes, to exhaustively quantify images on a cell-by-cell basis, and to investigate the statistical significance of the resulting numerical data in a hypothesis-independent manner. We expected that the results could quantify expected and unexpected effects of small molecules and provide information that was complementary to biochemical data.

As a test set to develop cytological profiling of small molecule action, we assembled 90 small molecules with known biological effects ("drugs"), choosing drugs expected to perturb human cancer cells in culture and including several groups of two to seven drugs with similar mechanisms. These included topoisomerase inhibitors, ribosome poisons, histone deacetylase inhibitors, microtubule poisons, and kinase inhibitors with various specificities. We added ten more drugs as blinded samples, choosing either drugs from the test set at different concentrations, or bioactive small molecules of unknown mechanism. These blinded samples were used to evaluate the success of our method. A key feature in the design of the experiment was dose-response information. Small molecules are expected to bind to more targets in cells as their concentration increases. Even for binding to a single target, various cell pathways may respond differentially to the degree of saturation of that target. Cell responses at a phenotypic level are thus expected to change, and become more complex, as dose increases. We used a concentration range of 66 pM–35 μM for each drug, which typically covered the range between no effect at the low dose and the onset of nonspecific effects at the high dose. We chose one time point (20 h) and one cell line (HeLa, a human cancer cell) to keep the study manageable. Additional time points and different cell types would add mechanistic information in future studies. The 20 hour time point is long enough that secondary responses to a drug could develop, mediated by transcriptional changes, for example. For the cytological-profiling experiment, cells were cultured in 384-well plates, treated with small molecules for 20 h, then fixed and stained with various fluorescent probes.

A key question in a profiling experiment of this kind is what probes to use, and what descriptors to collect. This question can be thought of in two ways, hypothesis-dependent and hypothesis-independent. In the former, one would choose probes and descriptors to look for specific biological effects that were expected in the experiment, such as toxicity, differentiation, mitotic arrest, etc. In the latter, one would choose a broad range of probes to cover both expected and unexpected biology, and measure as many descriptors as possible for each probe, without trying to predict which probe would be most useful, or which descriptors had known biological meaning. Because our drugs covered a large range of mechanisms, and because we hoped to detect "off-target" effects (effects due to perturbation of cell systems that do not correspond to the expected mechanism), we chose the hypothesis-independent approach. We selected probes somewhat arbitrarily so as to visualize a broad range of nuclear and cytoskeletal structures, as well as key signaling pathways (Figure 3, below). They included antibodies to phosphorylated states of signaling proteins, which provide information on pathway activity. For each probe, we collected all the single-cell descriptors that were easy to measure, including integrated fluorescence signal, average signal, variance of signal, cytoplasm-to-nucleus ratio, shape factors, number of spots, etc. In some cases the descriptor might have obvious biological meaning (e.g., integrated signal from the DNA stain DAPI, which measures DNA content per cell), and in other cases it might not (e.g. variance of DAPI signal). Our plan was to use clustering analysis to tell us retrospectively which probes and descriptors provided useful information on drug mechanism, and which did not. In practice we found that all the probes and descriptors were useful, and omitting any of them reduced the power of our analysis. We were surprised by this apparent nonredundancy of our descriptors, and further investigation is required to determine why descriptors with no obvious biological meaning are contributing useful data.

Using automated microscopy, we collected nine images per well (~8000 cells in total). This number was chosen so as to broadly sample each well, including the middle and sides, in case cell response was variable across the well. The cells were approximately confluent; this made it difficult to identify their outlines. Instead we identified individual nuclei, and then defined the cytoplasm as an annulus around each nucleus. For each cell and probe, we measured several descriptors that described fluorescence in the nucleus and cytoplasm, for a total of 93 descriptors from 11 probes. The full study was performed in duplicate and generated $\sim 10^9$ descriptor measurements in total. We then developed a statistical method to convert descriptor measurements into *Z*-scores for differences between a drug-treated well and control wells (DMSO-treated wells on the same 384-well plate) to normalize for any plate-to-plate variation in staining. These *Z*-scores were visualized as heat plots of *Z*-value versus drug concentration for each descriptor.

Figure 3 illustrates the heat plot for camptothecin, a topoisomerase inhibitor that caused DNA-strand breaks. To the left (low drug concentrations) most wells are the same as the control, with occasional colored pixels representing noise. As drug concentration increases, many descriptors become significantly different from the controls. This presentation allows us to visualize 93 separate dose-response curves in a single image, and we collected 100 such profiles in duplicate in the full study. For ~60 drugs that caused strong changes in a number of descriptors, the heat plot was very similar in the duplicate experiment, as measured by eye and by comparison of the duplicate sets by using unsupervised clustering, and we averaged *Z*-scores for further analysis. For ~40 drugs that caused few changes, the profiles were dominated by a small number of bright pixels at random positions. These were not reproducible between duplicates, and presumably represent noise introduced in processing or imaging the wells. These drugs either lack targets in HeLa cells, or perturbation of their targets did not cause biological effects that were detected by our probes. They were omitted from further analysis.

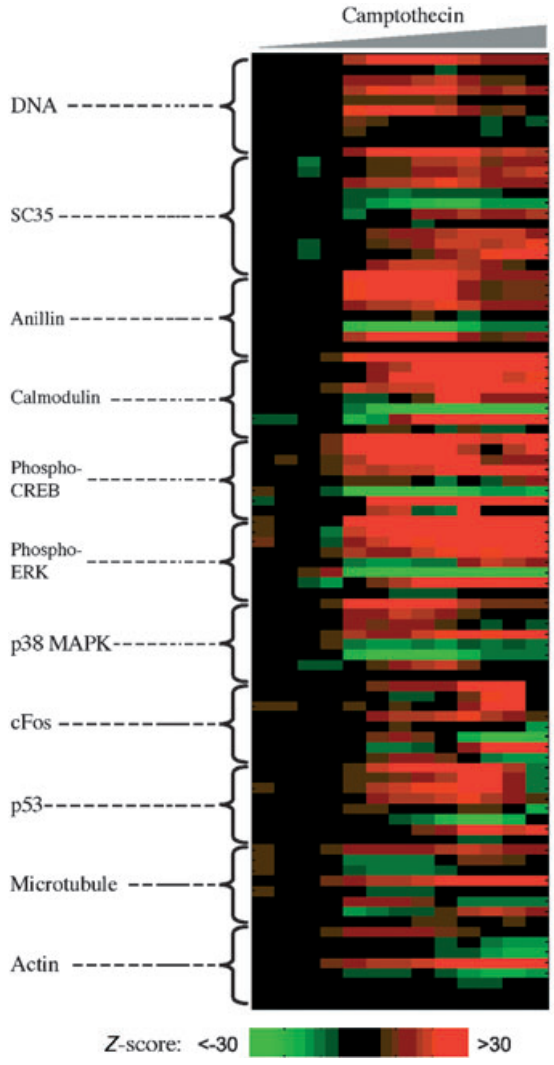

Figure 3. *Dose-response profile for campthothecin from a cytological-profiling experiment. This heat plot profiles the response of HeLa cells to increasing concentrations of the topoisomerase inhibitor camptothecin. On the y axis are a series of descriptors measured on a cell-by-cell basis. The text describes the macromolecule that the probes bind to. Fluorescent small molecules were used to detect DNA (DAPI) and actin (rhodamine-phalloidin). Antibodies labeled with fluorochromes were used in an indirect immunofluorescence protocol to detect the other proteins. Phospho-x refers to an antibody that binds specifically to a phosphorylated epitope on the protein. On the x axis are increasing drug concentrations (13 concentrations in a 3× dilution series from 66 pM to 35 μM). The color intensity represents the Z-score from a statistical test comparing descriptor values from cells in a treated well to cells in control wells on the same plate. Red indicates a positive deviation from control values, and green a negative deviation. Black indicates no statistically significant difference from controls. Each pixel in the heat plot represents the average Z-score for single wells from two duplicate experiments. For each well, nine nonoverlapping images were collected, and descriptors measured for ~8000 cells. Each well was stained with DAPI (blue channel) plus two other probes (green and red channels), so a single experiment required five sets of plates to cover all 11 probes. Note that at low drug concentrations most descriptors are not different from controls (Z-score~0), while at high drug concentration many descriptors are different from controls. The approximate EC_{50} value (potency) of the drug is that at which many descriptors change from like control to different. For details see ref. [14].*

The next issue was how to meaningfully compare profiles for different drugs. When comparing drugs, phenotypic effect and potency are separate issues. It is easy to measure potency from profiles like Figure 3, since the EC_{50} is simply the titration value at which many of the descriptors change from no different from control to significantly different. A sharp transition of this type was observed for all of the drugs that gave a strong signal (~60). To compare phenotypes while ignoring potency, we developed a titration-invariant similarity score (TISS), based on comparing pairs of heat plots over a series of left and right shifts on the concentration axis. The shift with maximum similarity was used to compute the TISS score, and the degree of similarity was used for unsupervised clustering (Figure 4). We then applied two criteria to test if our clustering had produced useful information. First, we asked if it had grouped together drugs that are known to have similar effects on cells, even though their structures are very different. The literature mechanism for each drug is annotated on the left in Figure 4, and success in grouping drugs by mechanism is demonstrated when boxes on one vertical line are grouped together. We were highly successful in clustering drugs with several mechanisms, including DNA damaging drugs, histone deacetylase inhibitors, and microtubule poisons. In one case, ribosome inhibitors, a group of related drugs that are potent and presumably fairly specific failed to cluster well. In this case, we suspect that the cell response to ribosome inhibition differs according to the detailed biochemical mechanism of each inhibitor. Second, we asked how well the blinded compounds (denoted by blue bars in Figure 4) clustered with their duplicate from the test set or with similar drugs, and found that eight out of eight of the blinded drugs of known mechanism did so. Since blinded drugs at one concentration clustered next to the same drug at a different concentration, this test demonstrates the success of TISS, and proves that we could infer mechanism of a novel drug if we had a similar drug to compare it to. For the two bioactive compounds of truly unknown mechanism, one (austocystin, a fungal poison) grouped with RNA and protein-synthesis inhibitors, and one (concentramide, a synthetic compound that perturbs zebrafish development) did not generate enough nonzero *Z*-scores to cluster; this suggests that HeLa

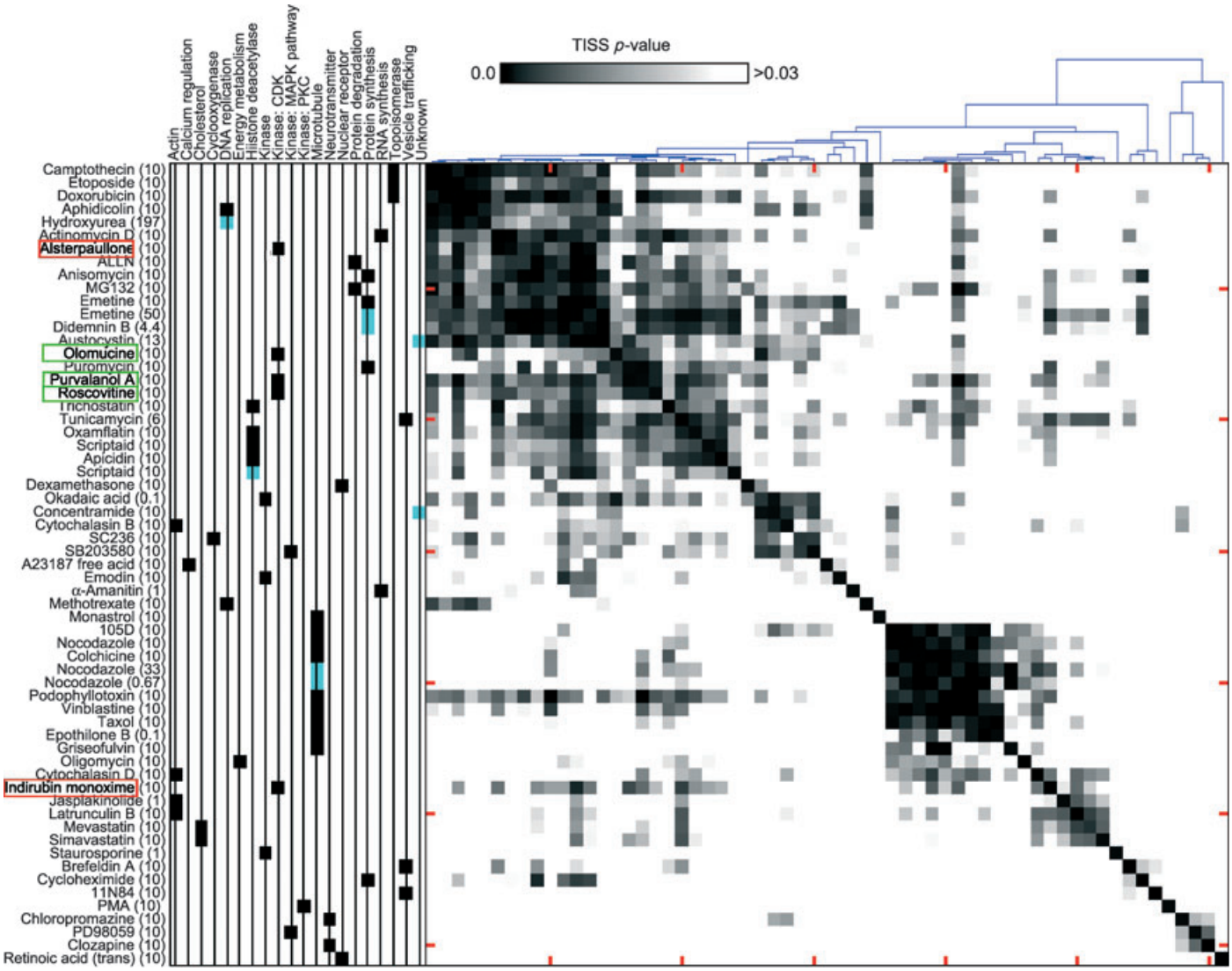

Figure 4. *Comparing phenotypic effects of drugs by clustering analysis. Dose-response profiles (as shown in Figure 3) for ~60 drugs that gave strong responses were compared by using an algorithm that measures similarity independently of potency (Titration Invariant Similarity Score). TISS scores were used for unsupervised clustering. A dendrogram of similarity is shown top right, and a matrix plot representing the TISS values for all pair-wise comparisons in the middle. Darker pixels indicate stronger similarity. In the line plot on the left, each drug is assigned to a mechanistic class according to the literature and manufacturer's information. Clustering of squares on a single line indicates success in grouping the drugs in that class. Note that the clustering succeeded in grouping together all members of several mechanistic classes, including topoisomerase inhibitors, histone deacetylase inhibitors, and microtubule drugs. The blue squares represent drugs that were blinded during the analysis, and used to measure success in clustering. The colored boxes indicate 5 cyclin-dependent kinase inhibitors whose structures are shown in Scheme 1. For details see ref. [14].*

cells might not express its target. Although this project is only a first effort toward systematic cytological profiling, we conclude that the approach will be useful for measuring drug efficacy and specificity at the level of cellular phenotype in both academic and commercial drug discovery.

To further illustrate the kind of information cytological profiling plus TISS provided in this experiment, consider the case of cyclin-dependent kinase (CDK) inhibitors. Five CDK inhibitors were included in our study, representing all of the drugs in this class sold by Calbiochem (Scheme 1). Because of strong homology in the kinase gene family, ATP-competitive kinase inhibitors typically inhibit a spectrum of different kinases, with different EC_{50}s; this makes therapeutic drug development in this area challenging. Kinase inhibitors are thus expected to show complex dose-response behavior at the phenotypic level, as increasing concentration causes inhibition of more kinases in the cell. Cytological profiling as a function of dose should be especially useful in measuring this kind of phenotypic complexity. In our study, three of the CDK inhibitors (green boxes in Figure 4 and Scheme 1) clustered close together; this indicated similar phenotypic effects as a function of dose, while two others (red boxes) clustered away from the green group and from each other. These data suggest that the green molecules share a similar spectrum of targets in the cell, while the red molecules have different target spectra. Inspection of the structures rationalizes this observation, since the green mole-

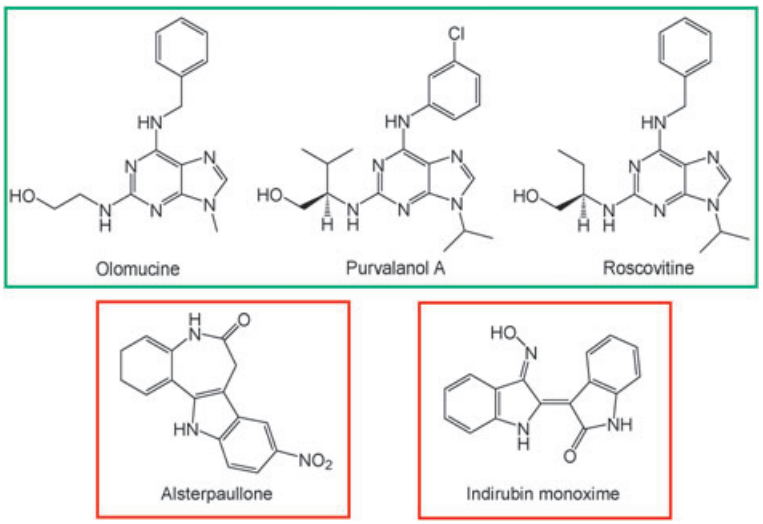

Scheme 1. *Structures of the five different cyclin-dependent kinase (CDK) inhibitors used in the cytological profiling study. The three drugs in the green box clustered close together (green boxes in Figure 4), while the two drugs in the red boxes clustered far from the green-box drugs and from each other (red boxes in Figure 4). Thus the green-box drugs had very similar phenotypic effects, while the red-box drugs had diverse effects. Note: the green-box drugs are similar to each other in structure, while the red-box drugs are structurally diverse.*

cules are highly related in structure, while the red molecules are quite different. In this case, phenotypic effects mapped to chemical structure in a predictable way, but it is easy to imagine a different result in a structure–activity experiment, with a small change in chemical structure causing a large change in phenotype. Data like those in Figure 4 and Scheme 1 could be useful during drug development, to relate biochemical measurements to phenotypic effects in structure–activity studies, a key step in early-stage therapeutic drug discovery.

Conclusion and Prospects

As the instrumentation for automated microscopy improves, it will become possible to collect larger data sets of high-quality images of fixed cells and also to image large numbers of cells expressing GFP-tagged proteins over time in order to observe dynamic behavior directly. Although many challenges remain, software for automated image analysis is also improving rapidly; this allows us to convert large data sets of cell images into numbers that can be used to score for a desired effect in screening applications, or to broadly describe cell phenotypes in profiling applications. What does the future hold in terms of discoveries that might be made with these technologies?

In the area of therapeutic drug discovery, it is clear that automated microscopy can be used effectively for primary high-throughput screening (HTS) of chemical libraries. Phenotypic screening is currently less popular than pure protein screening in commercial drug discovery, despite the fact that the initial leads for many therapeutic drug classes historically came from some kind of phenotypic information. The high information content of automated microscopy, the possibility of screening on small numbers of human primary cells, and the potential for discovery of new targets as well as new ligands make the technology worth considering for primary HTS. Cytological profiling, in which the number of small molecules investigated is smaller, but the information content is much higher, is well suited for the hit-to-lead phase of commercial drug discovery; here hundreds or perhaps thousands of small molecules must be evaluated rapidly for their potential to serve as leads for medicinal chemistry. It should be especially useful for relating biochemical activity to phenotypic effects in programs in which specificity is a challenge, such as kinase and histone deacetylase inhibitors. Cytological profiling provides information that is in principle complementary to other multidimensional profiling methods, such as transcript profiling,[16] comparison of cytotoxicity across multiple cell lines,[17] and synthetic interaction analysis.[18] Combing these types of data-rich analyses should help solve the difficult problem of predicting the biological effect of drugs prior to clinical trails.

Automated microscopy will be equally useful in scoring genetic- or pseudo-genetic screens, notably genome-wide RNAi screens that are now becoming feasible in *Drosophila* and human cells. The human genome contains ~25 000 genes, a small number by HTS standards, but large for conventional microscopy. We recently performed a screen for inhibition of cytokinesis, using small-molecule and genome-wide RNAi libraries in parallel, scoring for accumulation of binucleate cells.[8] Application of profiling methods to RNAi screens will add rich, quantitative annotation to databases of gene function. Perhaps the area where automated microscopy will have the largest impact is systems biology, the study of integrated behavior of whole biological pathways. Since systems biology is concerned with kinetic behavior of pathways in cells, and variation in response between different cells, analysis of individual cells over time is important, and automated microscopy makes this feasible across sample sizes that achieve statistical significance. Systems-level understanding will be essential if we hope to predict the effects of small molecules on cells (and people) in silico, and thus lower the time and cost of therapeutic drug discovery. Automated microscopy is only one of the tools that will be needed in the near future to improve the rate of discovery of bioactive small molecules, and their optimization into therapeutic drugs, but I hope this article makes the case that it will be an important one.

Acknowledgements

I thank all my co-workers on the projects described here, notably Steve Haggarty, Thomas Mayer, Tarun Kapoor, Justin Yarrow, John Hoyt, Shane Woods and Nicky Tolliday (mitosis screen), and Zach Perlman, Yan Feng, Mike Boyce, Lani Wu, and Steven Altschuler (cytological profiling). This work was supported by grants from NIH–NCI, NIH–GM, Merck, and Merck KGA.

Keywords: drugs · fluorescence · microscopy · profiling · screening

[1] R. A. Blake, *Curr. Opin. Pharmacol.* **2001**, *1*, 533 – 538.
[2] J. C. Yarrow, Y. Feng, Z. E. Perlman, T. Kirchhausen, T. J. Mitchison, *Comb. Chem. High Throughput Screening* **2003**, *6*, 279 – 286.
[3] V. Abraham, D. L. Taylor, J. R. Haskins, *Trends Biotechnol.* **2004**, *22*,15 – 22.
[4] B. R. Stockwell, *Nat. Rev. Genet.* **2000**, *1*, 116 – 125.
[5] T. U. Mayer, T. M. Kapoor, S. J. Haggarty, R. W. King, S. L. Schreiber, T. J. Mitchison, *Science* **1999**, *286*, 971 – 974.
[6] J. C. Yarrow, Z. E. Perlman, N. J. Westwood, T. J. Mitchison, *BMC Biotechnol.* **2004**, *4*, 21 – 28.
[7] S. Hotha, J. C. Yarrow, J. G. Yang, S. Garrett, K. V. Renduchintala, T. U. Mayer, T. M. Kapoor, *Angew. Chem.* **2003**, *115*, 2481 – 2484; *Angew. Chem. Int. Ed.* **2003**, *42*, 2379 – 2382.
[8] U. S. Eggert, A. A. Kiger, C. Richter, Z. E. Perlman, N. Perrimon, T. J. Mitchison, C. M. Field, *PLoS Biol.* **2004**, *2*, e379.
[9] Z. E. Perlman, T. J. Mitchison, T. U. Mayer, *ChemBioChem* **2005**, *6*, 145 – 151.
[10] Y. Feng, S. Yu, T. K. Lasell, A. P. Jadhav, E. Macia, P. Chardin, P. Melancon, M. Roth, T. Mitchison, T. Kirchhausen, *Proc. Natl. Acad. Sci. USA* **2003**, *100*, 6469 – 6474.
[11] N. Venkatesh, Y. Feng, B. DeDecker, P. Yacono, D. Golan, T. Mitchison, F. McKeon, *Proc. Natl. Acad. Sci. USA* **2004**, *101*, 8969 – 8974.
[12] T. R. Kau, F. Schroeder, S. Ramaswamy, C. L. Wojciechowski, J. J. Zhao, T. M. Roberts, J. Clardy, W. R. Sellers, P. A. Silver, *Cancer Cell* **2003**, *4*, 463 – 476.
[13] F. Gasparri, M. Mariani, F. Sola, A. Galvani, *J. Biol. Inorg. Chem. J. Biomol. Screen.* **2004**, *9*, 232 – 243.
[14] Z. E. Perlman, M. D. Slack, Y. Feng, T. J. Mitchison, L. F. Wu, S. J. Altschuler, *Science* **2004**, *306*, 1194 – 1198.
[15] J. M. Minguez, K. A. Giuliano, R. Balachandran, C. Madiraju, D. P. Curran, B. W. Day, *Mol. Cancer Ther.* **2002**, *1*, 1305 – 1313.
[16] D. J. Villeneuve, A. M. Parissenti, *Curr. Top. Med. Chem.* **2004**, *4*, 1329 – 1345.
[17] J. N. Weinstein, T. G. Myers, P. M. O'Connor, S. H. Friend, A. J. Fornace, Jr, K. W. Kohn, T. Fojo, S. E. Bates, L. V. Rubinstein, N. L. Anderson, J. K. Buolamwini, W. W. van Osdol, A. P. Monks, D. A. Scudiero, E. A. Sausville, D. W. Zaharevitz, B. Bunow, V. N. Viswanadhan, G. S. Johnson, R. E. Wittes, K. D. Paull, *Science* **1997**, *275*, 343 – 349.
[18] S. J. Haggarty, P. A. Clemons, S. L. Schreiber, *J. Am. Chem. Soc.* **2003**, *125*, 10543 – 10545.

Received: July 30, 2004

Early View Article
Published online on November 29, 2004

